Urol Res (2005) 33: 105–115
DOI 10.1007/s00240-004-0460-4

ORIGINAL PAPER

R. Corey O'Connor · Elaine M. Worcester
Andrew P. Evan · Shane Meehan · Dimitri Kuznetsov
Brett Laven · Andre' J. Sommer · Sharon B. Bledsoe
Joan H. Parks · Fredric L. Coe · Marc Grynpas
Glenn S. Gerber

Nephrolithiasis and nephrocalcinosis in rats with small bowel resection

Published online: 7 April 2005

Abstract Intestinal resection (IR) may lead to hyperoxaluria and nephrolithiasis. A rat model of IR was developed, in which kidney stones form. We describe the urine chemistries and histopathologic features. Rats underwent resection of 40–45 cm of distal ileum ($n = 16$) or sham resection (SR) ($n = 8$), and were then fed a 1% Na oxalate, 0.02% Ca diet. After 1 week on the diet, 24 h urine samples were obtained for stone chemistries. At 4–7 months after surgery, kidneys were examined grossly and by light microscopy. The extent and location of crystallization was assessed by polarized light. Histochemistry and infrared spectroscopy were used to determine crystal composition. IR rats had higher urine oxalate excretion ($P < 0.01$) and concentration ($P < 0.001$) than SR rats, and lower urine citrate excretion; only IR rats formed kidney stones (12/15 surviving rats). Tissue calcification was found only in kidneys from IR rats, located in the cortex (83% of kidneys), medulla (73%) and papillary tip (47%). Crystals, composed of CaOx, apatite, and calcium carbonate, filled collecting duct lumens, and were associated with tubular obstruction, and interstitial inflammation. Crystals in the papillary interstitium incited inflammation with tubular destruction and development of progressive papillary erosion. This new rat model of nephrolithiasis and nephrocalcinosis resembles the pattern of urinary abnormalities and tissue calcification that may be seen in humans with small bowel resection. The model allows further studies of the mechanisms of renal crystal formation, and possible therapeutic interventions.

Keywords Calcium oxalate · Hyperoxaluria · Kidney calculi · Small bowel resection

R. C. O'Connor · D. Kuznetsov · B. Laven · G. S. Gerber
Department of Urology, University of Chicago,
Chicago, IL, USA

E. M. Worcester (✉) · J. H. Parks · F. L. Coe
Department of Medicine, Nephrology Section,
University of Chicago, Chicago IL, USA
E-mail: eworcest@medicine.bsd.uchicago.edu
Tel.: +1-773-7021475
Fax: +1-773-7025818

S. Meehan
Department of Pathology, University of Chicago,
IL, USA

A. P. Evan · S. B. Bledsoe
Department of Anatomy and Cell Biology,
Indiana University School of Medicine,
Indianapolis, IN, USA

A. J. Sommer
Department of Chemistry and Biochemistry,
Miami University,
Oxford, Ohio, USA

M. Grynpas
Samuel Lumenfeld Research Institute,
Mt Sinai Hospital, Toronto, Canada

Introduction

Ileal resection (IR) or bypass in humans may lead to nephrolithiasis [1, 2, 3], and in some cases to renal damage [4, 5, 6], associated with crystallization of calcium oxalate (CaOx). The physiological basis for crystal deposition is complex, and includes reduced urine volume, citrate, and pH, and increased urine oxalate excretion [1, 7]. Reduced urine volume and pH appear to be direct consequences of fluid loss from diarrhea. Increased oxalate excretion appears to arise from excessive absorption of dietary oxalate in the colon [8, 9, 10]. CaOx nephrolithiasis has been estimated to occur in 15–30% of patients after intestinal bypass surgery, sometimes within months after the procedure; acute renal failure [11], renal tubular dysfunction [12], and chronic renal dysfunction [13] may also arise as complications. In addition, renal parenchymal scarring, with or without nephrocalcinosis, has been described in patients with hyperoxaluria biopsied up to 108 months after the

surgical bypass procedure [3]. The incidence of CaOx stones is also increased after small bowel resection, with onset averaging 8–10 years after surgery [7].

An animal model of CaOx urolithiasis secondary to IR could facilitate research into this well known human disease. In principle, IR should lead to hyperoxaluria because of increased colonic oxalate absorption. A prior attempt at a model of enteric hyperoxaluria in rats using jejunoileal bypass did not produce stones or hyperoxaluria, although urinary supersaturation with respect to CaOx increased via increased urine calcium, an unexpected result [14]. In reviewing this work, we noticed that the diet was relatively high in calcium and low in oxalate. Since high calcium in the diet can reduce urine oxalate in humans [15], we hypothesized that a model of enteric hyperoxaluria secondary to bowel resection might lead to stones if dietary oxalate was increased and calcium reduced. We also considered that increased dietary lipid might foster oxalate absorption by increasing the supply of fatty acids [1]. We report here the successful development of a rodent model of IR with consequent hyperoxaluria, CaOx urolithiasis and renal crystallizations that resemble those seen in human disease and other animal models of oxalate deposition disease.

Methods and materials

Animals and surgical technique

Male Sprague-Dawley rats, weighing 180–200 g, and acclimated to a room temperature of 25°C, with a 12-h light/dark cycle, were fed a standard diet until 24 h prior to surgery, at which time the diet was removed and they had free access to a solution containing 25 g of dextrose in 500 ml of water. Anesthesia was performed using an intraperitoneal injection of a 0.3–0.5 ml solution of Ketamine (90 mg/kg), atropine (0.05 mg/kg) and Xylocaine (10 mg/kg). Following the administration of anesthesia, the animals were secured and the abdominal area was shaved of fur and sterilely prepared with 70% ethanol and Betadine paint. A midline laparotomy was performed. Control rats underwent transection of the distal ileum without excision of any intestine, followed by re-anastomosis. Resection rats underwent removal of the distal 40–45 cm of small intestine measured from the ileocecal valve, followed by re-anastomosis of the small intestine. In a subset of rats, the distal 40–45 cm of small intestine was resected along with the ileocecal valve, followed by re-anastomosis of the proximal small bowel to the cecum. This latter was done in order to be sure we had removed all of the most terminal ileum. We found that the two resection procedures led to indistinguishable results in terms of urine chemistries and renal histopathology, and pooled the results from these animals. In all animals, hemostasis during surgery was accomplished using electrocautery with an average blood loss of less than 1 ml. Following completion of surgical anastomosis, 12 ml of normal saline was instilled in the peritoneum and the abdomen was closed using 3–0 silk suture. The rats received buprenorphine 0.01–0.05 mg subcutaneously every 8–12 h for the first 24 h as post operative analgesia.

All animals were given standard rat chow (5.7% lipid) beginning 8 h after surgery. This continued until the animals regained their preoperative weight, which generally occurred by 7–10 days following surgery. The animals were then placed in individual cages and fed 15 g of the experimental diet, which contained 1% sodium oxalate, 0.02% calcium and 18% lipids in pellet form daily. The 15-g portions of food assured equal and complete consumption of the diet by each animal during every 24-h period and allowed for continued growth of the rats. The rats were maintained on this diet until they were killed.

Animal experiments were carried out in accordance with the NIH Guide for the Care and Use of Laboratory Animals.

Urine collection and measurements

Nalgene metabolic cages were used for the 24-h urine collections. One ml of 4 N HCl and 250–500 mg. of thymol (Fisher Scientific, Hanover Park, Ill., USA) were added to the collection container at the onset of collections. A urine sample was collected after 1 week on the experimental diet. Thymol prevents bacterial overgrowth and 4 N HCl allowed for complete measurement of urinary oxalate by preventing formation of calcium salt precipitates and in vitro oxalate production. The 24-h urine collections were analyzed for volume, calcium, oxalate, citrate, creatinine, phosphorus, sodium, potassium, magnesium, ammonia, and sulfate, using techniques described elsewhere [16].

Light microscopic histology

Animals were killed and the kidneys removed at 4, 5, 6 and 7 months after surgery; four resected rats and two sham operated rats were killed at each time point, except that one resected rat in the 7 month group died prior to this time. Each rat kidney was inspected, bivalved and any loose calculi were saved. The kidneys were fixed by immersion in 10% neutral buffered formalin. Each kidney was embedded in paraffin and 4-μm sections were stained using hematoxylin and eosin. Representative sections were stained using the Jones methenamine silver method to delineate the tubular basement membranes. The silver rubeanate method [17] was used to identify calcium oxalate, phosphate and carbonate containing salts.

Quantitative microscopic evaluations

Two independent observers (A.E. and S.M.M.) assessed the extent of crystal accumulation in separate anatomic

Table 1 Initial urine measurements (1 week)

	Resected	Sham
n	16	8
Oxalate (mg/d)	5.4 ± 0.6	3.3 ± 0.3[b]
Oxalate (mM/l)	7.9 ± 1.1	1.9 ± 0.2[c]
Citrate (mg/d)	2.1 ± 0.4	3.6 ± 0.5[a]
Citrate (mM/l)	1.6 ± 0.4	1.0 ± 0.1
Calcium (mg/d)	0.3 ± 0.1	0.34 ± 0.05
Calcium (mM/l)	0.9 ± 0.2	0.48 ± 0.08[a]
CA x OX mM^2	8 ± 2	1.0 ± 0.2
Magnesium (mg/d)	3.3 ± 0.2	3.2 ± 0.2
Volume (ml/d)	9 ± 1	18 ± 2[c]
Creatinine (mg/d)	6.9 ± 0.4	11.8 ± 0.7[c]
Phosphate (mg/d)	18 ± 1	21 ± 2
Sodium (mM/d)	0.8 ± 0.1	1.4 ± 0.1[c]
Potassium (mM/d)	0.6 ± 0.05	0.7 ± 0.1
Ammonia (mM/d)	0.6 ± 0.2	0.5 ± 0.2
Sulfate (mM/d)	0.5 ± 0.2	0.6 ± 0.2
Body weight (gm)	260 ± 57	343 ± 22[c]

[a] vs resected, $P < 0.05$, [b] $P < 0.01$, [c] $P < 0.001$

compartments including renal pelvic lumen, pelvic wall, cortex, medulla and papilla. Partially and fully polarized light was used to highlight birefringent crystal deposits. The extent of crystallization was semi-quantitatively evaluated using a subjective scoring system where 0 = none, 0.5 + = few, 1 + = several and 2 + = many crystal deposits. Tubular ectasia accompanied by interstitial inflammation, with or without rupture and extrusion of proteinaceous material into the interstitium, was interpreted as evidence of intrarenal tubular obstruction.

Infrared spectroscopy

Tissue sections from two animals in the 4 month surgical group and two from the 4 month sham operated group were analyzed by Fourier transform infrared microspectroscopy (μ-FTIR) to determine the mineral composition of the sites of crystal deposits. Infrared spectra were collected with a Perkin-Elmer Auto Image infrared microscope interfaced to a Perkin-Elmer Spectrum 2000 Fourier transform spectrometer (Perkin-Elmer, Shelton, Conn., USA) in the Molecular Micro-spectroscopy Laboratory of Dr. Andre' J. Sommer, Department of Chemistry and Biochemistry, Miami University, Oxford, Ohio. Analysis was performed according to our previously published protocol [18].

Electron diffraction and energy dispersion analysis

Tissue prepared for TEM containing two inner medullary collecting ducts with crystal deposits were studied. Electron diffraction was performed with a Philips TECNAI 20 at 100 kV and with a diffraction camera length of 890 mm. The sample was routinely prepared

Table 2 Histopathological grading of kidney tissue. For gross calculi and obstruction: 0 = absent, 1 = present; for crystals 0 = none, 0.5 = few, 1 = several, 2 = many. Proliferation indicates tubular epithelial proliferation without detectable crystal formation

Time of death	Pelvic lumen		Pelvic urothelium	Papilla	Medulla	Cortex	Obstruction
	Gross	Microscopic					
4 months	1	0.5	1	No sample	0.5	0.5	1
	1	0.5	0.5	0.5	0.5	0.5	1
	1	1	1	0.5	0.5	0.5	1
	0	1	0	Proliferation	0.5	0	1
	1	0.5	0.5	1	0.5	0.5	1
	1	0.5	0.5	1	0.5	0.5	1
	1	0.5	0	0.5	0.5	0.5	1
	1	0.5	0.5	Proliferation	0.5	0.5	1
5 months	0	0	0	0	0	0	0
	0	0	0	0	0	0	0
	1	1	0	0	1	0.5	1
	0	0.5	0	0	0	0	1
	0	0.5	0	0	0.5	0.5	1
	0	0	0	0	0	0.5	1
	0	0.5	0.5	Proliferation	0	0.5	1
	1	1	0	0	0.5	1	1
6 months	1	0	1	No sample	0	0.5	1
	1	0.5	0.5	0.5	0.5	0.5	1
	0	0.5	1	0.5	0.5	0.5	1
	0	0.5	0.5	0.5	0.5	0.5	1
	1	1	1	1	2	2	1
	1	1	1	2	2	2	1
	0	0	0.5	0	0	0	1
	1	1	0.5	0	0	0.5	1
7 months	1	0	0	No sample	0.5	1	1
	1	1	1	2	1	1	1
	1	1	2	0.5	0.5	0.5	1
	1	1	1	0.5	0.5	0.5	1
	1	2	1	0.5	0.5	0.5	1
	1	0.5	0.5	No sample	0.5	0.5	1

for TEM analysis but not stained. The energy dispersive x-ray analysis was performed with the Phoenix EDAX instrument.

Data analysis

Urine measurements from resected or sham-operated animals were compared using *t*-tests. All analyses used conventional statistical software (Systat, Richmond, Calif).

Results

Urine chemistries

Compared with sham animals, resection led to increased urine oxalate and reduced urine citrate excretions (Table 1). Urine oxalate molarity was increased by both hyperoxaluria and reduced urine volume. These urine changes would be expected to cause stones. In the non-resected rats fed the high oxalate diet there were neither

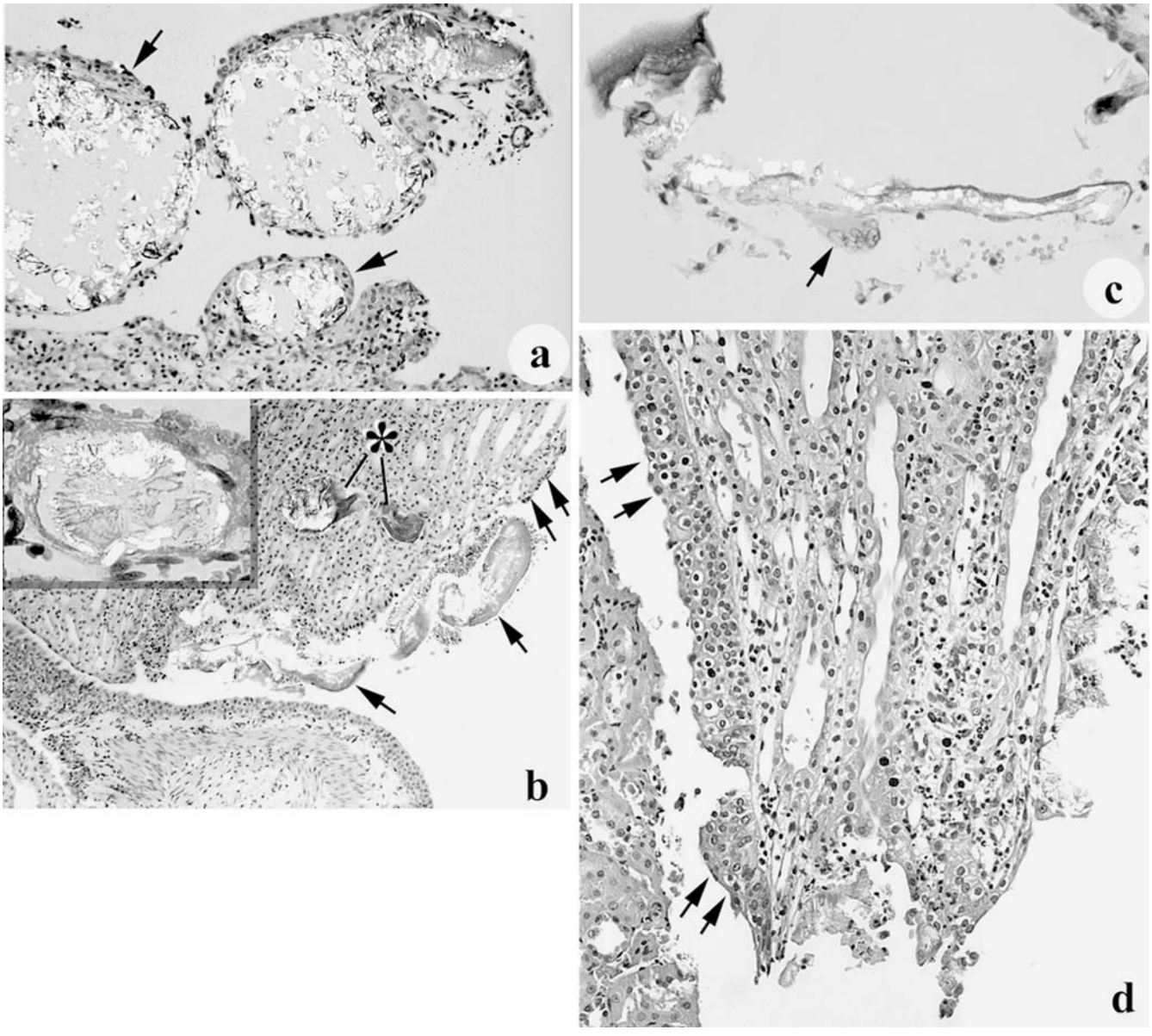

Fig. 1 Light micrographs showing that the outermost surface of the pelvic calculi had deeply basophilic laminated material with (a, arrows) or without (b, arrows) an epithelial lining. The central portions of these larger intrapelvic protein-crystal aggregates (PCA) consisted of sheaves of birefringent crystals. Similar intraluminal crystal deposition of calcium phosphate (non-birefringent center) and calcium oxalate (birefringent outer layer) was noted in inner medullary collecting ducts (b asterisk, insert). c Illustrates the smallest of the pelvic luminal PCA with an attached giant cell (arrow). d Shows an animal from the 4-month group that demonstrates papillary crystallization with tissue necrosis, an acute inflammatory response as well as ectasia of some medullary collecting ducts. Transitional epithelial hyperplasia was commonly noted at sites of pelvic crystal accumulation (a, d) (double arrows). Magnification ×30 (a); ×75 (b); ×250 (inset b); ×250 (c), ×60 (d)

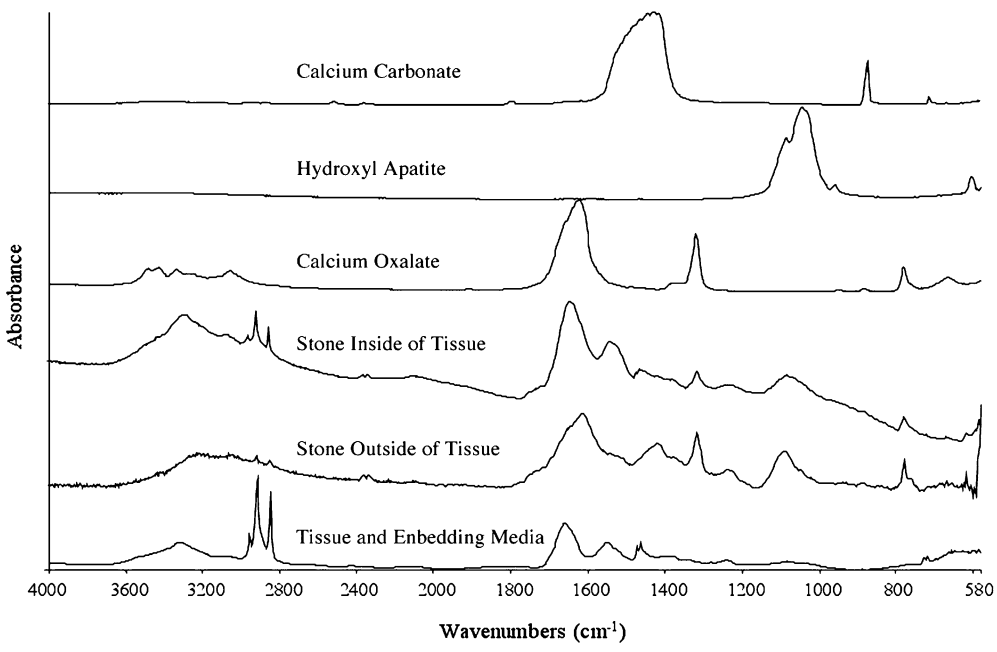

Fig. 2 μFTIR spectra of crystal deposits in the inner meduallary collecting ducts and renal pelvis of the rats with intestinal bypass surgery. This figure illustrates a series of infrared spectra obtained for a set of standards (calcium carbonate, CaOx and hydroxyapatite), for a site of calcium deposit (Yasue-positive area) in the renal pelvis and in the lumen of an inner medullary collecting duct as well as for the tissue-embedding medium. The infrared spectra for both Yasue-positive areas show a spectral band for hydroxyapatite and calcium oxalate. Occasionally a spectral band for calcium carbonate was found

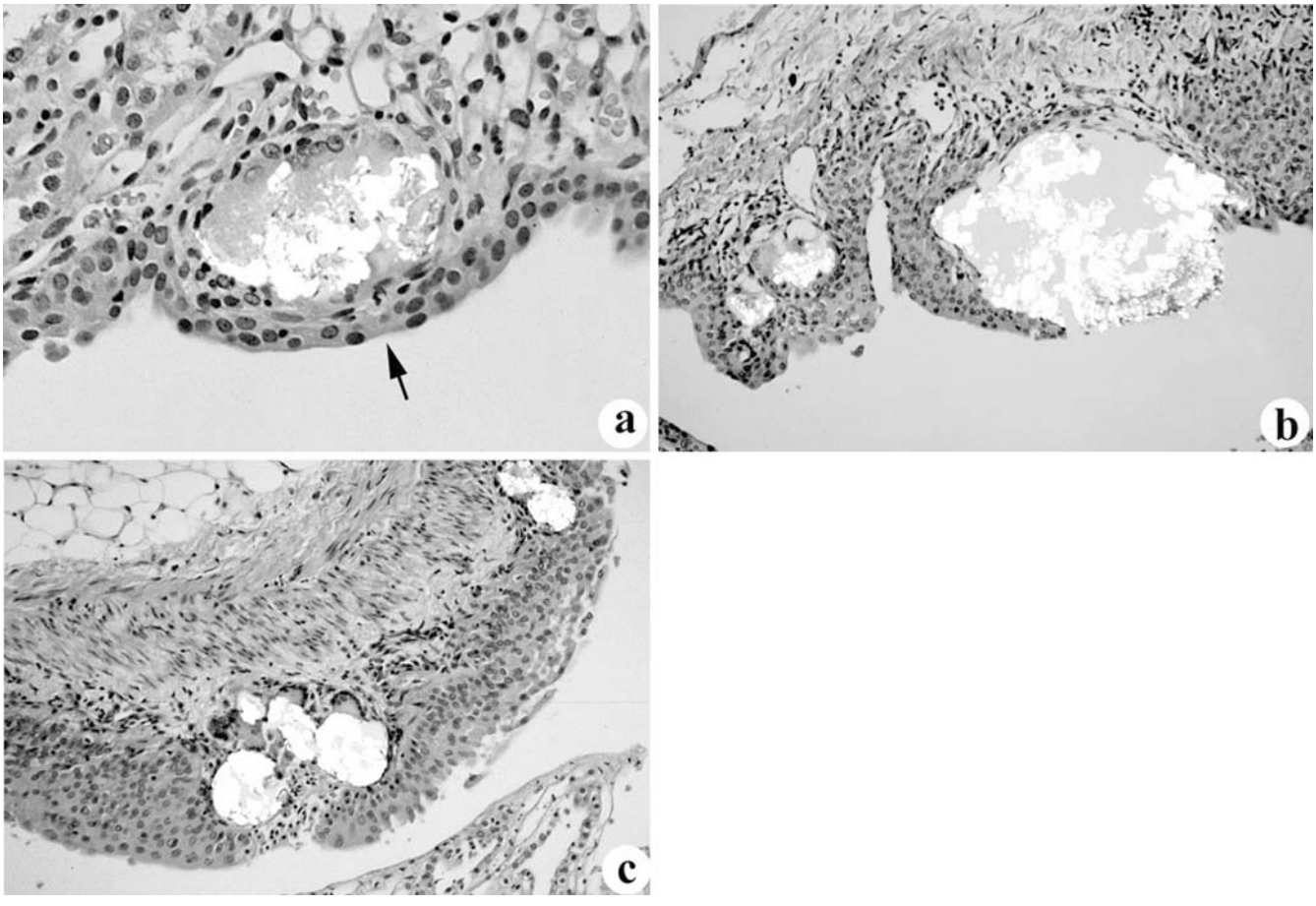

Fig. 3 Light micrographs showing calcium oxalate and hydroxyapatite accumulation at the urothelium. a Shows crystal entrapment within a proliferative urothelium (arrow) at the fornix. B, C

stones nor crystals in any of the kidneys. Tissue architecture was completely normal and is not further reported here.

Histological changes in the 15 resected animals

Twelve of the 15 surviving resected rats formed stones, and had renal tissue abnormalities (Table 2). Although we had hoped that kidneys with the least amount of crystal deposition might provide an opportunity to identify the sites of early crystallization, we found generalized crystal deposition already present by 4 months, which means we can not detect the sequence of crystallization in this study. Stones were already present in the 4-month rats.

Pelvic lumen

Loose, grossly identifiable calculi, measuring approximately 0.5–2 mm, were observed in the renal pelvis in 20 of 30 kidneys from resected animals (12 of 15 resected rats). Gross calculi were unilateral in four and bilateral in eight rats. Six further kidneys had microscopic aggregates of crystals identifiable in the pelvis as detached masses of crystals associated with what appears to be proteinaceous material (proteinaceous crystal aggregates, PCA), giving a total of 26 of 30 kidneys (87%) with pelvic lumen crystal accumulation. By light microscopy, the outermost surfaces of larger PCA had deeply basophilic laminated material with (Fig. 1A) or without (Fig. 1B) an epithelial lining. The central portions of the large PCA consisted of sheaves of birefringent crystal. By infrared spectroscopy of seven PCA, the

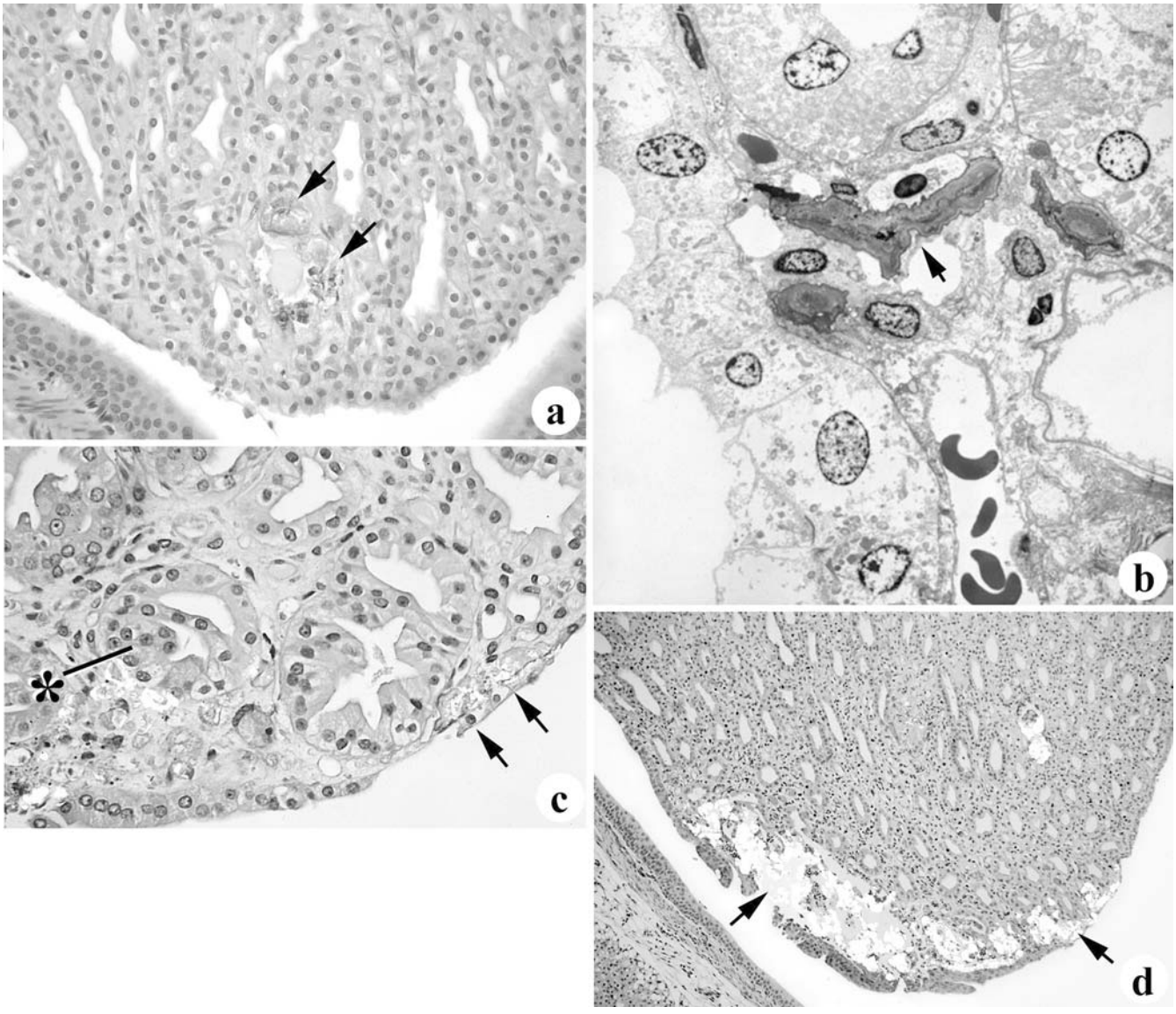

Fig. 4 Crystal deposition at the papillary tip in a 7 month animal. Crystal accumulation (arrow) in lumens of the inner medullary collecting ducts was one of the earliest changes noted in these kidneys (a). These crystal deposits usually resulted in cell necrosis of adjacent lining cells (a) and hyperplasia (asterisk) of nearby tubules (c). Crystal accumulation (arrows) also occurred in the interstitium near tubules as seen in the TEM micrograph in b or beneath the urothelium (c, d, arrows). Magnification, ×60 (a); ×4,950 (b); ×120 (c); ×25 (d)

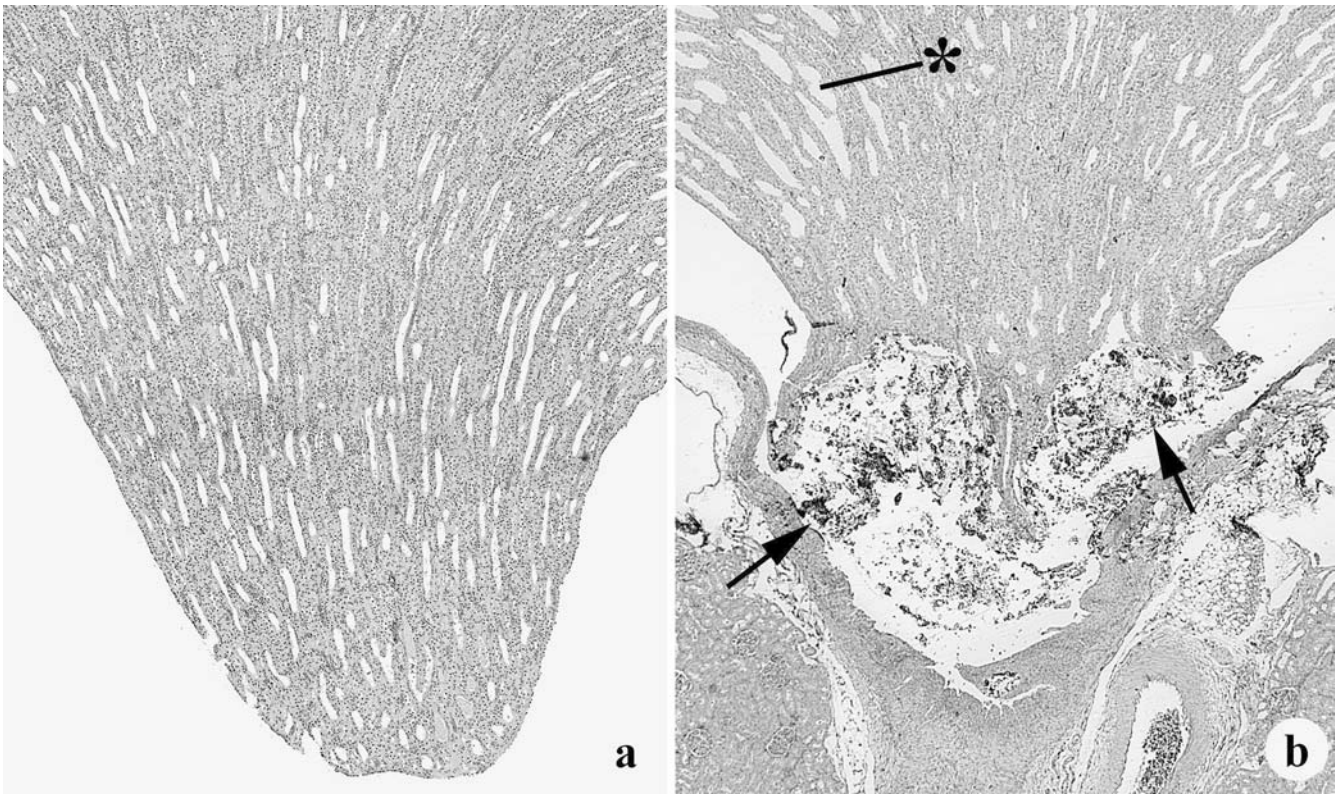

Fig. 5 Comparison of papillary tip from 4 month control (a) vs 4 month intestinal bypass animal (b). Erosion of the papillary tip with large crystal accretion of the surgically treated animal is obvious compared to the control. Areas of crystal deposition (arrows) replaced normal tubular and interstitial architecture. Ectasia (asterisks) of the collecting duct system progressed from the inner medulla to the cortex (b). Magnification, ×12 (a); ×12 (b)

crystals were composed of a mixture of calcium carbonate, hydroxyapatite and oxalate (Fig. 2). The smallest intra-pelvic luminal birefringent crystals were attached to strands of basophilic matrix material which appeared to float freely (Fig. 1C) in the pelvis and occasionally were observed attached to multinucleated giant cells. The matrix material appeared to form the framework for the accumulation of larger quantities of birefringent crystal. Similar appearing material was observed in the epithelial layer and immediately beneath the epithelium of the fornix and pelvic wall. Larger crystalline aggregates were located deep in the pelvis and were associated with transitional epithelial hyperplasia (Fig. 1B, 1D).

Renal pelvic wall

The deepest portions of the pelvic fornix and the basal papillary surface frequently had subepithelial crystal accumulation with formation of pseudopapillary projections from the pelvic and papillary surface (Figs. 1A, 3A). Molded crystalline aggregates were noted in the fornices (not shown). Basophilic fibrillar laminated material with birefringent crystals were observed in giant cells that localized in the subepithelial zone or within the transitional epithelium (not shown). Intraepithelial birefringent crystals within giant cells were also observed (Fig. 3A–C). Intraepithelial crystals were associated with transitional epithelial hyperplasia (Fig. 3A–C) in the pelvis and ureter and with transitional metaplasia of the papillary surface epithelium (Fig. 1D).

Renal papilla

Crystals accumulated in the lumens of the inner medullary collecting ducts (Bellini ducts) (Figs. 1B, 4A, D) and in the interstitium beneath the papillary surface epithelium (Fig. 4B–D). Intralumenal crystal deposits in the ducts of Bellini contained both calcium phosphate and calcium oxalate (Fig. 1B, insert) and were associated with and often preceded by hyperplasia of the Bellini duct epithelium (Fig. 4C). Tubules filled with crystal aggregates had epithelial necrosis or apoptosis (Fig. 4A). Crystal accumulation in the tubule lumens was associated with larger regions of calcium phosphate and oxalate accumulation in the interstitium beneath the papillary surface and adjacent to the involved tubules (Fig. 4B–D).

Crystallization also occurred eccentrically on the papillary slope away from the tip, and involved the tubules and interstitium. Interstitial birefringent crystals incited an acute inflammatory response with margination of neutrophils and mononuclear inflammatory cells in the interstitial capillaries, and exudation into the interstitium adjacent to the crystals (Fig. 4C, D). One kidney had subepithelial plaque-like deposits (Fig. 4D). Tissue necrosis was evidenced by eccentric erosion of the

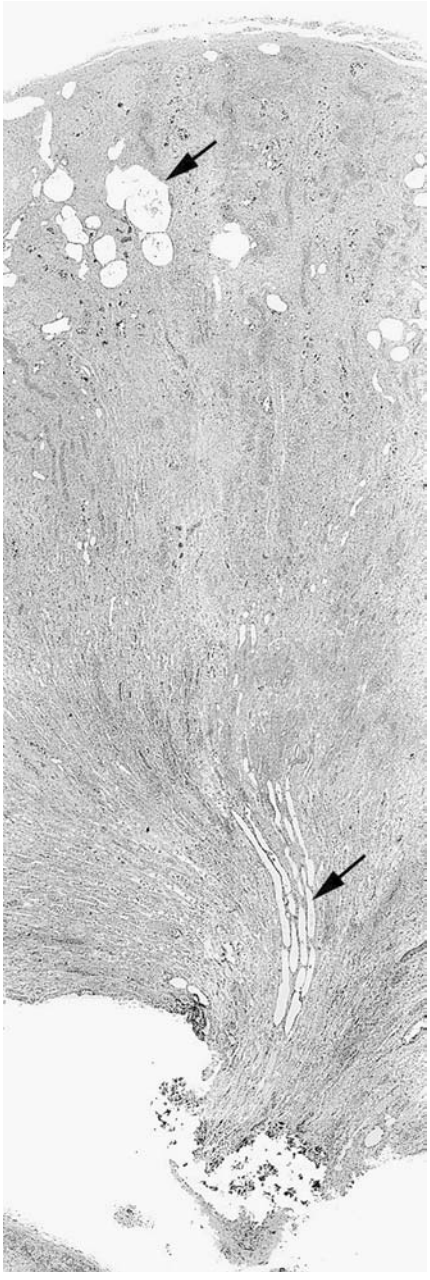

Fig. 6 Changes in the renal papilla were associated with injury to the cortical tissues. This figure shows the advanced changes noted in a 6-month kidney. Almost half of the renal papilla has been eroded away. Collecting duct ectasia is prominent in both the medulla and cortex (arrows). Tubular atrophy, interstitial inflammation and crystal accumulation is also present but is difficult to see at this low magnification. Magnification, ×5

papillary tips associated with large papillary tip crystal accretion (Fig. 5A, B). ''Calculi'' measuring 1–2 mm were firmly attached to the papillary tips in 9/30 kidneys from resected rats.

Renal cortex and medulla

Crystal accumulation in the cortex was associated with collecting duct ectasia. Ectasia extended from the medulla to the cortex, with focal (Fig. 1B), to diffuse involvement of the cortex (Fig. 6). Crystals were found in lumens of injured tubules and in tubular epithelium (Fig. 7A), and were extruded into the cortical interstitium, sometimes within a proteinaceous matrix, but more often as small clusters of crystals in multinucleated giant cells. Collecting duct obstruction was associated with interstitial inflammation, tubular atrophy and interstitial fibrosis (Fig. 7A, B) resulting in retraction of the cortical surface.

Nature of the crystal deposits

Two of the 20 loose calculi were analyzed and were composed solely of CaOx monohydrate by standard infrared spectroscopy. A total of 20 separate inner medullary collecting ducts containing crystal deposits were studied by μ-FTIR spectroscopy. CaOx was found in every one. In 15 of the 20, CaOx was associated with definitive spectral bands of hydroxyapatite. Calcium carbonate was definitively present in one of the 15. In the other five tubules, spectral bands were suggestive but not definitive for hydroxyapatite. Seven PCA contained CaOx, as well as definitive evidence for hydroxyapatite. Using TEM in two kidneys, very small crystal deposits (1–30 μm) were found in the inner medullary interstitium. All contained electron dense, laminated crystalline material, and were adjacent to basement membranes of collecting ducts. We conjecture these may be calcium phosphate because of their morphological appearance. Two deposits in inner medullary collecting ducts in tissue processed for TEM were studied by electron diffraction (Fig. 8) and energy dispersive x-ray analysis (Fig. 9). In both, poorly crystallized CaOx could be identified, but hydroxyapatite could not be identified. Carbonate was not identified.

Discussion

The present results support our initial hypothesis that ileal resection in rodents will produce urolithiasis and renal crystallization if diet calcium is reduced and oxalate increased sufficiently. Our animals are hyperoxaluric with low urine volume and citrate. They produce calcium oxalate uroliths, and develop severe renal crystal deposition disease. The urine chemistries seen in the resected rats on the high oxalate diet are similar in many respects to those seen in humans with small bowel resection who have formed stones, studied on their ordinary diet [7]. For these reasons, the model offers new opportunities for research.

Relationship of pathological changes to human disease

Certain of the pathological changes we describe here have been found in kidneys of patients with short bowel

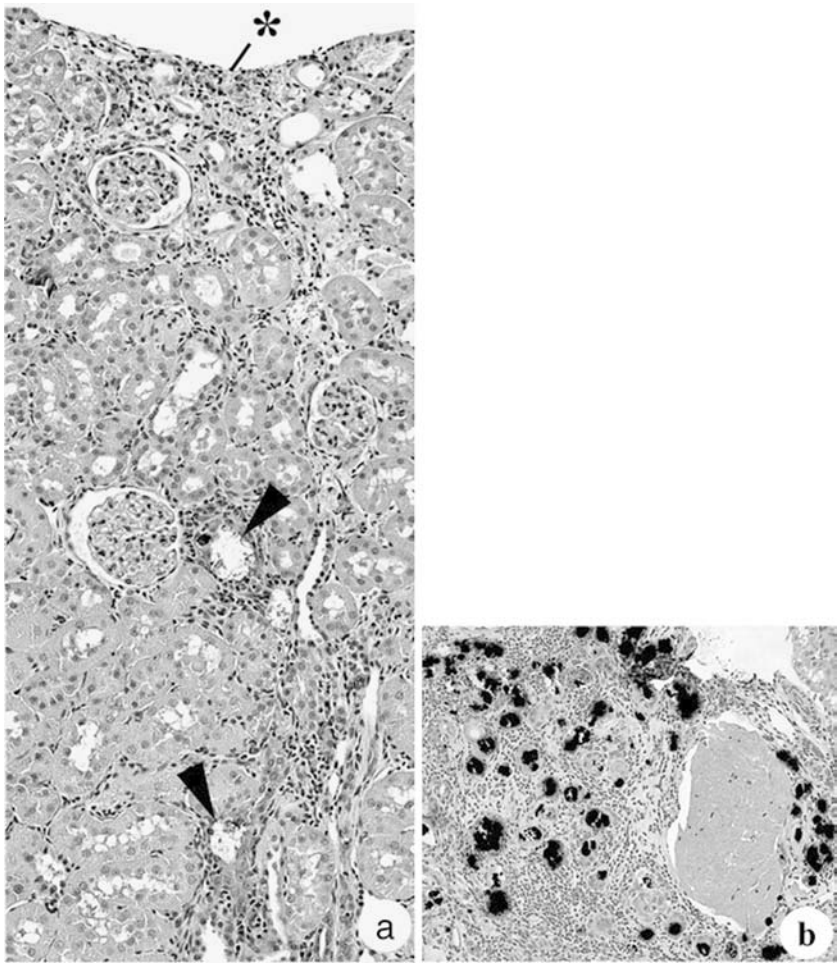

Fig. 7 **a** Shows a higher magnification light micrograph of a region of tubular atrophy that extends from the renal capsule (asterisk) to the corticomedullary junction. Crystal accumulation is noted in a few damaged tubules (arrowheads). **b** Shows numerous sites of crystal accumulation by the Yasue method for the identification of Ca deposits (black areas). Cortical crystal deposition appeared to be localized to sites of tissue injury. Magnification, ×45 (**a**); ×80 (**b**)

or bypass procedures [4, 11, 13, 18, 19, 20, 21, 22], not all of whom formed stones. When stones form, they are usually CaOx, with little or no admixed calcium phosphate [7]. We have described four patients with intestinal bypass procedures who formed stones [18]. All had well preserved renal function with minimal changes

Fig. 8 Electron diffraction pattern of crystalline deposit in lumen of a medullary collecting duct. This diffraction pattern is indistinct and very broad indicating that the deposit is a poorly crystalline substance. The measurement of the d-spacing is about 2.8 A indicating the presence of a calcium oxalate phase

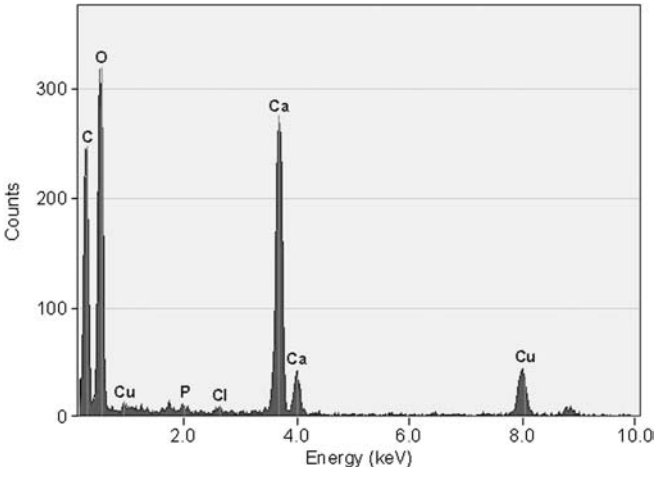

Fig. 9 Energy dispersive x-ray (EDX) analysis of the same crystalline deposit referenced in Fig. 8. The major elements are calcium, carbon and oxygen. Only trace amounts of phosphorous were detected

in the kidney, except for plugging of some inner medullary collecting duct lumens with hydroxyapatite crystals [18]. These crystals could represent loss of normal acidification in collecting ducts. Others have described more advanced lesions in patients with bowel disease, some of whom had lost significant kidney function. These include tubulointerstital lesions together with significant deposits of crystals in the cortex, identified as CaOx by polarization [4, 11, 21, 22], infrared spectroscopy [13], or X-ray diffraction studies [13, 19]. Crystals were associated with significant acute and chronic tubular injury, inflammation and fibrosis. The pattern of change in the renal cortex of these patients is similar to what we found here in cortical tissue. Of course, by design, human kidney biopsies rarely reveal inner medullary tissue, so that the lack of past descriptions of human papillary changes in patients with overt renal functional deficits is expected.

One form of renal crystallization described here requires special comment. We found crystal deposits of CaOx and hydroxyapatite in the interstitial suburothelial compartment at the papillary tip. We did not find this in our human biopsies. We believe collecting duct injury and interstitial inflammation and necrosis result in secondary crystallization of the papillary tip. A second crystallization, seemingly peculiar in this model but possibly a form of Anderson-Carr body [23], consists of deposits of CaOx and hydroxyapatite beneath and within the urothelium, in the forniceal regions. We do not understand the pathogenesis of this lesion. The suggestion of a primary lymphatic involvement [23] probably does not apply given the location of the lesions in our model.

Comparison to other animal models

Some renal changes in our animals match those described in other models of hyperoxaluria. In particular, crystal deposition in the cortex and papillary changes such as ours are well described as a consequence of ethylene glycol [24]. Tubular atrophy and interstitial fibrosis are well-known consequences of crystal deposition with cell injury [25]. On the other hand, some changes here are not usually described. Cortical collecting duct ectasia, which was a consistent observation in our animals, is not characteristic of other hyperoxaluric rodent models. The urothelial changes found here that resemble Anderson-Carr bodies also occur in inbred hypercalciuric rats rendered hyperoxaluric by feeding with hydroxyproline [16], but have not been described in other rodent hyperoxaluric models. We found that crystals were admixtures of calcium oxalate, and hydroxyapatite, in most regions of crystal deposition, whereas calcium oxalate has generally been the sole crystal described in the renal tissues of other rodent hyperoxaluric models. Finally, when rats are merely fed a high oxalate diet, no crystals or stones are found, showing the importance of the resection in the model [26]. What is most different, of course, is etiology. The fact that ileal resection can lead to a consistent pattern of stones and nephrocalcinosis affords new research opportunities to explore a situation that resembles an established and not uncommon human disease.

The finding of definitive spectral bands for hydroxyapatite in 15/20 inner medullary duct deposits and suggestive bands in the other five duct deposits makes us reasonably certain that this phase is present in these tissues. This is supported by our finding of H-E positive crystals by light microscopy and the crystalline pattern by TEM. On the other hand, lack of confirmation in the two tubules studied by electron diffraction and energy dispersion indicates a need for further study of this matter. Given definitive evidence for hydroxyapatite in 15/20 ducts, the two may have differed because of simple sampling variability.

The primary effects of the high oxalate low calcium diet presumably arise from the augmented oxalate absorption in the gut, but other aspects may be important. The diet is very low in calcium, which certainly promotes oxalate absorption [27]. Possibly, vitamin deficiencies may occur over time because of malabsorption. The low calcium diet, by contrast, must certainly promote increases in calcitropic hormone levels [28] These are matters that are as yet unexplored.

Summary

Ileal resection combined with a high oxalate high fat low calcium diet reproducibly leads to calcium urolithiasis and renal crystallization in a pattern resembling human enteric hyperoxaluria. Urine and tissue changes resemble those of humans with this disease. Although many differences are present between human disease and this model, the model offers potential opportunities for research into this specific human disorder.

Acknowledgements This study was supported by NIH NIDDK PO1 56788 and the Department of Urology, University of Chicago, Chicago, IL. It was previously published in abstract form in 2004 in J Urol 171: S297

References

1. Worcester EM (2002) Stones from bowel disease. Endocrinol Metab Clin North Am 31: 979
2. Gelzayd EA, Breier RI, Kirsner JB (1968): Nephrolithiasis in inflammatory bowel disease. Am J Digest Dis 13: 1027
3. Obialo CI, Clayman RV, Matts JP, Fitch LL, Buchwald H, Gillis M, Hruska KA (1991) Pathogenesis of nephrolithiasis post-partial ileal bypass surgery: case-control study. The POSCH Group. Kidney Int 39: 1249
4. Drenick EJ, Stanley TM, Border WA, Zawada ET, Dornfeld LP, Upham T, Llach F (1978) Renal damage with intestinal bypass. Ann Intern Med 89: 594
5. Hassan I, Juncos LA, Milliner DS, Sarmiento JM, Sarr MG (2001) Chronic renal failure secondary to oxalate nephropathy: a preventable complication after jejunoileal bypass. Mayo Clin Proc 76: 758

6. Mole DR, Tomson CRV, Mortensen N, Winearls CG (2001) Renal complications of jejuno-ileal bypass for obesity. Q J Med, New Ser 94: 69
7. Parks JH, Worcester EM, O'Connor RC, Coe FL (2003) Urine stone risk factors in nephrolithiasis patients with and without bowel disease. Kidney Int 63: 255
8. Earnest DL, Johnson G, Williams HE, Admirand WH (1974) Hyperoxaluria in 9atients with ileal resection: an abnormality in dietary oxalate absorption. Gastroenterology 66: 1114
9. Dobbins JW, Binder HJ (1997) Importance of the colon in enteric hyperoxaluria. N Engl J Med 296: 298
10. Modigliani R, LaBayle D, Aymes C, Denvil R (1978) Evidence for excessive absorption of oxalate by the colon in enteric hyperoxaluria. Scand J Gastroenterol 13: 187
11. Ehlers SM, Posalaky Z, Strate RG, Quattlebaum FW (1977) Acute reversible renal failure following jejunoileal bypass for morbid obesity: a clinical and pathological (EM) study of a case. Surgery 82: 629
12. Vainder M, Kelly J (1976) Renal tubular dysfunction secondary to jejunoileal bypass. JAMA 235: 1257
13. Gelbart DR, Brewer LL, Fajardo LF, Weinstein AB (1977) Oxalosis and chronic renal failure after intestinal bypass. Arch Intern Med 137: 239
14. Blaurock P, Schwille PO, Manoharan M, Scheele J, Fries W, Rumenapf G (1992) Effects of jejunoileal bypass on oxalate and mineral metabolism in rats. Eur J Surg 158: 595
15. Stauffer JQ (1977) Hyperoxaluria and intestinal disease: the role of steatorrhea and dietary calcium in regulating intestinal oxalate absorption. Dig Dis 22: 92
16. Bushinksy DA, Asplin JR, Grynpas MD, Evan AP, Parker WR, Alexander KM, Coe FL (2002) Calcium oxalate stone formation in genetic hypercalciuric stone forming rats. Kidney Int 61: 975
17. Yasue T (1969) Histochemical identification of calcium oxalate. Acta Histochem Cytochem 2: 83
18. Evan AP, Lingeman JE, Coe FL, Parks JH, Bledsoe SM, Shao Y, Sommer A, Paterson R, Kuo R, Grynpas MD (2003) Randall plaque of patients with nephrolithiasis begins in basement membranes of thin loops of Henle. J Clin Invest 111: 607
19. Canos HJ, Hogg GA, Jeffery JR (1981) Oxalate nephropathy due to gastrointestinal disorders. CMA J 124: 729
20. Zawada ET, Johnston WH, Bergstein J (1981) Chronic interstitial nephritis: its occurrence with oxalosis and anti-tubular basement membrane antibodies after jejunoileal bypass. Arch Pathol Lab Med 105: 379
21. Hicks K, Evans GB, Rogerson ME, Bass P (1998) Jejuno-ileal bypass, enteric hyperoxaluria, and oxalate nephrosis: a role for polarized light in the renal biopsy. J Clin Pathol 51: 700
22. Wharton R, D'Agati V, Magun AM, Whitlock R, Kunis CL, Appel GB (1990) Acute deterioration of renal function associated with enteric hyperoxaluria. Clin Neph 34: 116
23. Carr RJ (1953) A new theory on the formation of renal calculi. Br J Urol 26: 105
24. Khan SR, Hackett RL (1985) Calcium oxalate urolithiasis in the rat: is it a model for human stone disease? A review of recent literature. Scan Electron Microsc 1985 part 2: 759
25. DeWater R, Noordermeer C, Vanderkwast T, Nizze H, Boeve ER, Kok DJ, Schroder FH (1999) Calcium oxalate nephrolithiasis: effect if renal crystal deposition on the cellular composition of the renal interstitium. Am J Kidney Dis 33: 761
26. Bushinsky DA, Bashir NA, Riordon D, Nakagawa Y, Coe FL, Grynpas MD (1998) Increased dietary oxalate does not increase urinary calcium oxalate saturation in hypercalciuric rats. Kidney Int 55: 602
27. Barilla DE, Notz C, Kennedy D, Pak CY (1978) Renal oxalate excretion following oral oxalate loads in patients with ileal disease and with renal and absorptive hypercalciurias. Effect of calcium and magnesium. Am J Med 64: 579
28. Coe FL, Favus MJ, Crockett T, Strauss AL, Parks JH, Porat A, Gantt CL, Sherwood LM (1982) Effects of low-calcium diet on urine calcium excretion, parathyroid function and serum 1,25(OH)2D3 levels in patients with idiopathic hypercalciuria and in normal subjects. Am J Med 72: 25